Solar Energy Materials & Solar Cells 106 (2012) 71–75

Contents lists available at SciVerse ScienceDirect

Solar Energy Materials & Solar Cells

journal homepage: www.elsevier.com/locate/solmat

Rating and sorting of mc-Si as-cut wafers in solar cell production using PL imaging

Jonas Haunschild*, Isolde E. Reis, Teodora Chipei, Matthias Demant, Benjamin Thaidigsmann, Michael Linse, Stefan Rein

Fraunhofer Institute for Solar Energy Systems ISE, Heidenhofstr. 2, 79110 Freiburg, Germany

ARTICLE INFO

Available online 7 June 2012

Keywords:
Photoluminescence imaging
mc-Si wafer quality
Wafer rating

ABSTRACT

Photoluminescence (PL) imaging is a promising characterization technique for rating and sorting of multicrystalline silicon (mc-Si) as-cut wafers concerning to their material quality. It is inline applicable and yields high resolution images showing recombination active defects from crystallization which influence solar cell performance. In this contribution the basic concepts in ongoing work concerning relevant defects, rating results, statistics, algorithms and general approaches for the rating are summarized. Since 2009 wafers are sorted into five quality classes at Fraunhofer ISE. Details on the rating criteria are given and three examples for application are presented: (i) the impact of edge contaminations on the solar cell results, (ii) a comparison of wafer suppliers based on random samples from a statistical basis of 10,000 wafers and (iii) the results of an advanced rating and sorting of wafers for the manufacturing of highly efficient MWT-PERC solar cells. The results confirm that PL imaging can be used for a very precise rating of material quality.

1. Introduction

Recently, it has been shown that photoluminescence (PL) imaging is an efficient tool for wafer quality control of mc-Si [1–3] and Cz-Si [4] as-cut wafers. The method can be used to detect material defects in as-cut wafers during incoming quality control before solar cell production, which allows rejecting wafers with too low quality.

Various companies are working on inline inspection systems and have published promising results on large numbers of mc-Si solar cells. In addition, McMillan et al. [5] have given an overview over practical and theoretical aspects, while True et al. [6] discussed the speed of different algorithms for feature extraction. Nagel [7] and Birkmann et al. [8] had their focus in theoretical and empirical modeling of the influence on solar cell results of different defect categories and Bakowskie et al. [9] compared the PL images of as-cut wafers with reverse-biased EL images.

In this study, we will summarize the basic defect categories of mc-Si which can be observed in PL images of as-cut wafers and explain the rating approach. The basic rating and sorting which is performed at the PV-TEC (Photovoltaic Technology Evaluation Center) at Fraunhofer ISE since 2009 will be presented and three examples for application will be given: (i) the impact of the defect feature of edge regions, (ii) a comparison of three wafer suppliers based on 10,000 mc-Si wafers and (iii) the application of an advanced rating for highly efficient MWT-PERC solar cells.

* Corresponding author. Tel.: +49 4588 5563; fax: +49 4588 9250.
E-mail address: jonas.haunschild@ise.fraunhofer.de (J. Haunschild).

0927-0248/$ - see front matter © 2012 Elsevier B.V. All rights reserved.
http://dx.doi.org/10.1016/j.solmat.2012.05.027

2. Approaches for PL imaging based wafer rating

2.1. Correlation to global solar cell parameters

In all publications on PL imaging based wafer rating, specific image features are extracted from the PL images of as-cut wafers and compared to IV parameters (V_{OC} or J_{SC}) of the finished solar cells so far. To set up a reliable prediction, lots of wafers for training purposes are needed. This task is in particular difficult, because there are different superimposing defects present in mc-Si wafers which can affect solar cell performance differently. In addition, the rating results strongly depend on how the defect features are defined and on the image processing algorithms which are used to extract the different defect features from the images. Typically there is no detailed information on the algorithms given because they are confidential intellectual property of the companies. Demant et al. [10] will describe a more advanced defect feature analysis, while results and examples for a basic rating and sorting following the approach of global correlation are presented below.

2.2. Basic defect categories

PL images taken on as-cut wafers show many material defects resulting from the crystallization process. In general, three main categories of defects may be distinguished:

- Wafers from corner and edge regions of the crucible show reduced carrier lifetimes due to in-diffusion of metallic contaminations from the crucible wall into the ingot. Typically, the affected area decreases with increasing ingot height. These impurities can partly be gettered during emitter diffusion, but the gettering efficiency strongly depends on the chosen diffusion process. Thus, the impact of this defect category on the solar cell parameters depends on the underlying solar cell process.

- Wafers from top and bottom regions of the brick show reduced carrier lifetime due to in-diffusion of metallic contaminations from the crucible wall into the ingot (bottom region) and due to segregation of these impurities up to the top of the ingot. A rating is difficult because impurities can partly be gettered during emitter diffusion.
- Crystal defects e.g. grain boundaries, twins or dislocations appear as lines or clusters in the images and reduce carrier lifetime in their vicinity. While impurities from the previous categories can be gettered or cut-off, crystal defects cannot be cured during solar cell processing and thus are the most relevant defect for wafer rating.

More details can be found in Ref. [1,5].

3. Basic rating and sorting

Following the approach of global correlation and based on the results presented in Ref. [1,2], a PL-based wafer rating was established at the PV-TEC at Fraunhofer ISE at the end of 2009. Five quality classes have been defined according to the area fraction of the basic defect categories. In Fig. 1 a representative image of each class is shown and the accepted maximum area fraction for each defect is given below (in percent of the total wafer area). Class 1 comprises premium wafers which can be used for high efficiency processing. Usually, these rare wafers can be found in the lower parts of center bricks where dislocations and contaminations are lowest. In class 2, we accept slightly more dislocations and all wafers from corner and edge regions because these contaminations can be gettered rather well. Class 3 wafers are up to date the most frequent ones, exhibiting medium fractions of different kinds of defects. Class 4 and 5 are rejected from solar cell processing as large fractions of dislocations and contaminations can influence the solar cell results significantly.

Please note that as stated above, the extracted area fraction strongly depends on the applied image processing algorithm. Details on the algorithm used here can be found in Ref. [1].

4. Results and discussion

4.1. Example 1: influence of edge contaminations

In the first example, it is shown, how differences in material quality can be identified in the PL images of as-cut wafers and be rated with respect to solar cell performance. Fig. 2 shows the PL images. In Fig. 3 the impact of corner and edge areas on solar cell efficiency is displayed in comparison to center wafers on a batch of standard screen-printed solar cells. 10 wafers per group were chosen from the same height of different ingot positions. In this way it can be assumed that the impact of the edge feature is not overruled by other material defects.

It is obvious that efficiency increases with decreasing amount of contaminated regions, the difference between center and edge brick being rather small. The reason might be a limitation by the applied solar cell process or an overruling impact from a slightly increased amount of dislocations ranging from 5% to 10% area fraction in this set of wafers. Note, that an inline P-diffusion has been applied. Thus the negative influence of the corner and edge areas, can be more evident as it would be in the case of a standard $POCl_3$ diffusion.

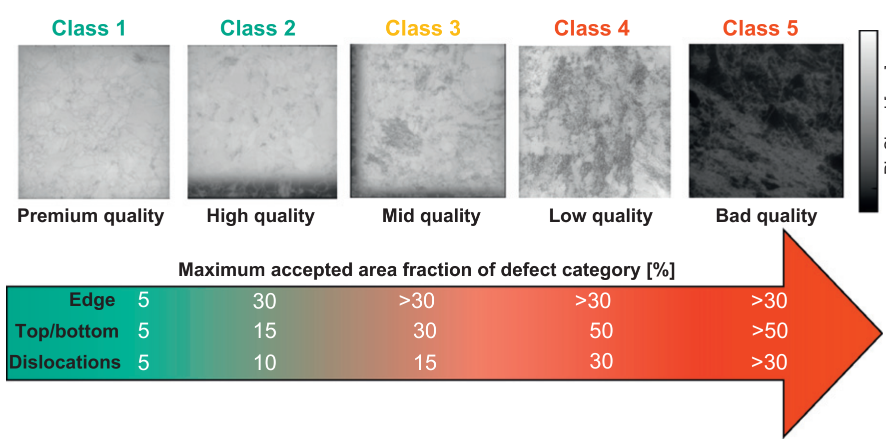

Fig. 1. PL images of as-cut wafer rated in class 1 to 5 (images from left to right). From class 1 to 5 the fraction of edge, top/bottom region and the dislocation density are increasing. The defect with the highest fraction is the crucial one for rating.

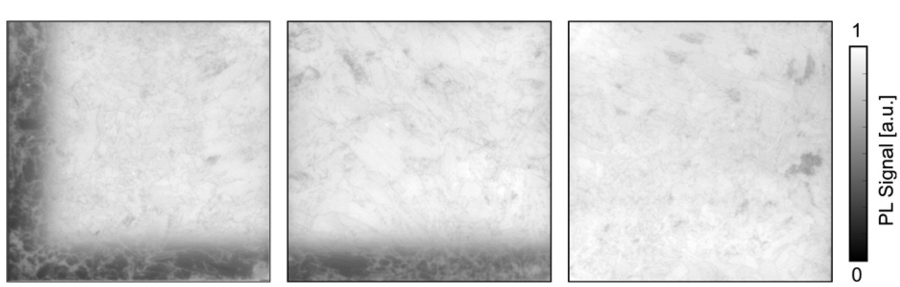

Fig. 2. PL images of typical wafers from a corner (left), edge (mid) and center (right) region.

4.2. Example 2: comparison of wafer suppliers

In the second example, the result of a comparison of different wafer suppliers is presented. In October 2011 approximately 10,000 mc-Si wafers from three different suppliers were delivered and pre-characterized by means of PL imaging. The measurement of the total number of wafers could not be realized with the manual PL imaging tool, so the PL testing was performed systematically on random samples containing 5–10% of the wafers from each of the approx. 100 wafer boxes with 50–175 wafers each. Each of the wafer boxes contains several stacks of neighboring wafers which can be identified easily by their grain structure. As crystal defects do change slowly over ingot height, it is sufficient to measure every 25th wafer of each stack within a box and to assign the rating result to its neighboring wafers of the same stack as well. In total 57 stacks of neighboring wafers were identified for supplier 1, 73 for supplier 2 and 126 for supplier 3. Images of 2 to 4 wafers per stack were taken resulting in a total number of 699 measurements. The quality of the wafers has been classified into one of the above described five categories.

Fig. 4a–c shows the rating results for each of the three suppliers separately. It is obvious that the portion of wafers in each quality class varies significantly among the suppliers. About a third of the wafers from supplier 1 are class 1 and 2 wafers, another third are class 3 and the last third are class 4 and 5 wafers which need to be rejected from solar cell processing. In contrast to that, the highest amount of class 1 and 2 wafers was delivered by supplier 2, i.e., 77% of the wafers are suitable for high efficiency processes, while 19% are still assigned to class 3 and only 4% failed the test. Supplier 3 delivered only corner wafers, which is why there is no top-class rating for this supplier. But as the density of dislocations is very low, almost 75% of wafers are rated into class 2. Good results should be achieved by applying an adapted solar cell process where the highly contaminated corner region can efficiently be gettered. The remaining wafer from supplier 3 are rated into class 3 (approx. 20%) and only 7% together into class 4 and 5.

The wafers from supplier 1 have overall the lowest quality but they are as well 25% cheaper than the wafers from supplier 2 and 3. Moreover, the wafers from supplier 2 are even slightly more expensive than those from supplier 3. Thus, the quality distribution matches more or less to price in this case.

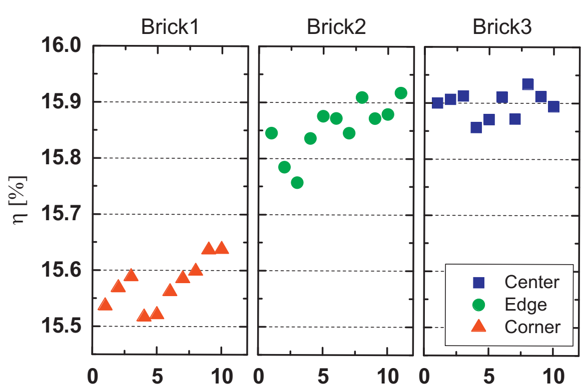

Fig. 3. Solar cell efficiencies achieved by a standard solar cell process with an inline P-diffusion for three different bricks from corner, edge and center regions.

4.3. Example 3: MWT-PERC solar cell results

The rating results presented in Section 4.1 are based on standard screen-printed solar cells. The limitation of the solar cell process to efficiencies of 16 to 17% makes it hard to identify differences in material quality in the top class categories 1 and 2. Advanced solar cell concepts might react more sensitive to differences in material quality, which enables a more detailed wafer rating.

For a special high-efficiency experiment, only top category wafers have been selected from the wafer stock at Fraunhofer PV-TEC to ensure highest solar cell efficiencies. To test a more precise rating, the classes 1 and 2 have been subdivided into three sub-quality levels: class A^+, having lowest amount of dislocations and contaminations (both below 5%), class A, having slightly more dislocations (max. 10%) and almost no contaminations (max. 5%), and class B^+, having more contamination (max. 10%), but very few dislocations (max. 5%). Wafers from all three sub-classes are processed in parallel to MWT-PERC solar cells [11]. Fig. 5 shows PL images which are representative for the three sub-classes.

To check the sorting result, a small reference group was processed prior to the main experiment of 1100 wafers. The results of the main experiments are overruled by process variations and thus cannot be evaluated concerning material related aspects. Fig. 6 shows the efficiency, short circuit current and open circuit voltage values of the cells from this reference group. It is obvious that for the class A+ (16 wafers) η, J_{SC} and V_{OC} are the highest, followed in quality by the class A (22 wafers) and then the class B+ (15 wafers) as predicted in advance.

The results confirm that even a more detailed rating for top category wafers is possible for high efficiency processes. The challenge is to implement the small differences in defect features into sorting algorithms which are fast enough for inline application.

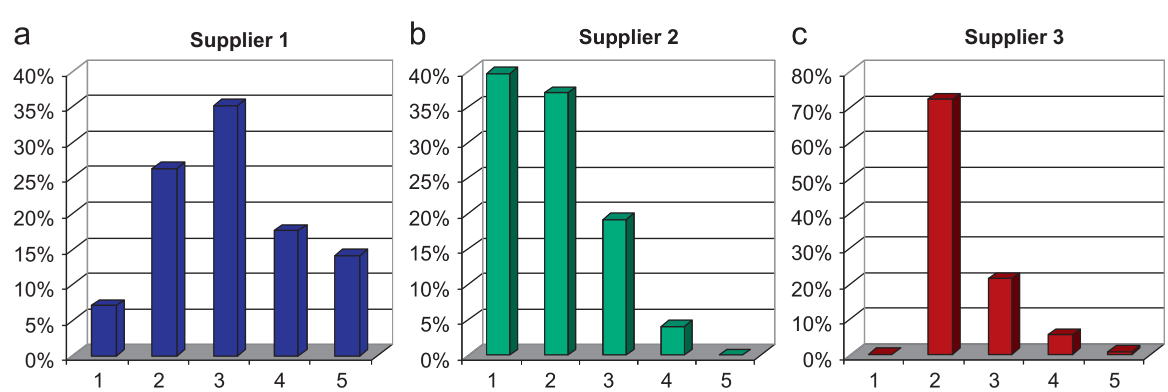

Fig. 4. (a) Most of the wafers are covered by strong dislocations, and are thus rated to class 3 or even class 4 or 5.Only 33% of the wafers were rated to be good enough for an industrial solar cell production. (b) All wafers are center wafers with very few crystal defects, e.g., dislocations, especially the high portion of class 1 wafers can be used to produce solar cells with highest efficiencies. (c) All investigated wafers were corner wafers with partly large extension of the contaminated region. A good result is the low percentage of low quality wafers.

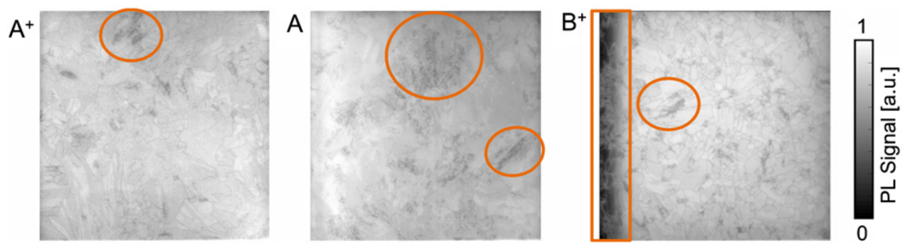

Fig. 5. Examples for PL images of as-cut wafer of the three top level categories A^+, A and B^+. While A^+ wafers show lowest amount of contaminations and dislocations, more dislocations are allowed in class A and more contaminations are allowed in class B^+.

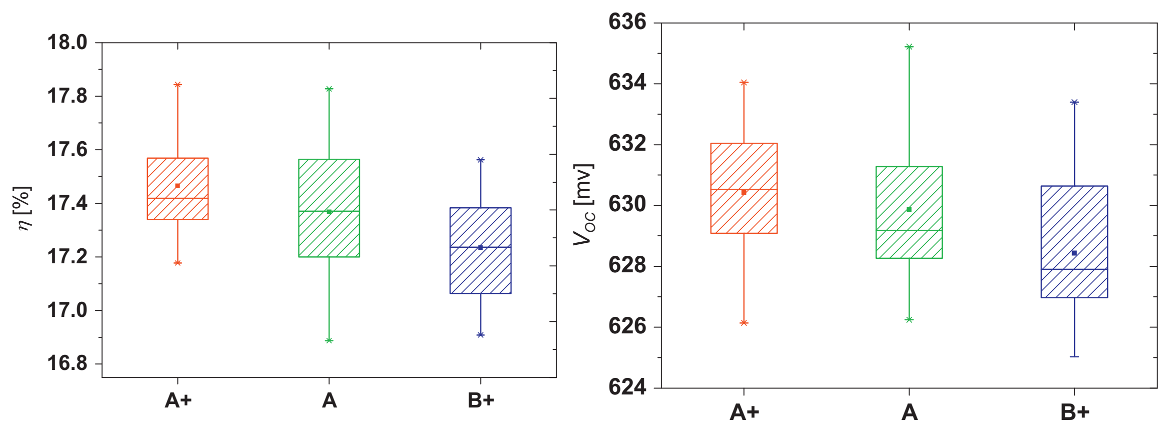

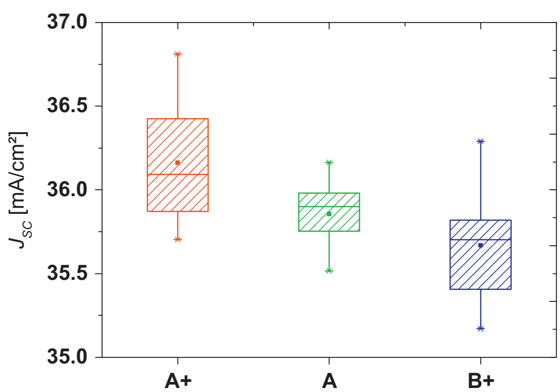

	A^+ (15 wafers)	A (22 wafers)	B^+ (16 wafers)
η [%]	17.5 ± 0.2	17.4 ± 0.3	17.2 ± 0.2
V_{OC} [mV]	630 ± 2.1	629 ± 2.3	628 ± 3.2
J_{SC} [mA/cm²]	36.2 ± 0.4	35.9 ± 0.2	35.7 ± 0.3
FF [%]	76.6 ± 0.2	76.9 ± 0.8	76.9 ± 0.8

Fig. 6. Efficiency η (top left), J_{SC} (bottom left), V_{OC} (top right) and the corresponding *I–V* data of the processed reference MWT-PERC cells depending on the classification performed in advance in the as-cut state by means of PL imaging.

5. Conclusion

By means of photoluminescence imaging, as-cut multicrystalline silicon wafers are rated with respect to the defect density, the fraction of edge/corner and the fraction of bottom/top contamination, respectively, and then categorized into five quality classes depending on the highest amount of one of these defects. This procedure is applied at Fraunhofer ISE since 2009. A comparison of three wafer suppliers shows big differences in material quality of commercially available material labeled to be high quality on a statistical basis of 10,000 wafers. Approximately one third of all wafers from supplier 1 had to be rejected from solar cell processing, while supplier 2 had almost no rejects and a high amount of top-class wafers and supplier 3 delivered wafers from corner ingots with very low dislocation density. Standard solar cell processing limits the achievable results in a way that small differences in material quality of top-class wafers cannot be detected anymore. The results of an advanced sorting of top-class wafers for a highly efficient MWT-PERC process confirms that even small differences in material quality have an effect on the *I–V* data. Thus incoming inspection based on PL imaging can be used as a powerful tool for quality control for both standard and advanced solar cell concepts.

Acknowledgments

The authors would like to thank all co-workers at the Photovoltaic Technology Evaluation Center (PV-TEC) at Fraunhofer ISE for cell processing. This work has partly been supported by the Fraunhofer Society under the frame of the project “ABICS-LUM” and by the German Ministry for Education and research (BMBF) under the frame of the project “Q-Wafer” (03SF0409A).

References

[1] J. Haunschild, M. Glatthaar, M. Demant, J. Nievendick, et al., Quality control of as-cut multicrystalline silicon wafers using photoluminescence imaging for solar cell production, Solar Energy Materials and Solar Cells 94 (2010) 2007.
[2] T. Trupke, J. Nyhus, J. Haunschild, Luminescence imaging for inline characterisation in silicon photovoltaics, Physica Status Solidi RRL 5 (2011) 131.

[3] M. Demant, J. Haunschild, M. Glatthaar, S. Rein, Analysis of luminescence images applying pattern recognition techniques, in: Proceedings of the 25th EU-PVSEC, Valencia, Spain, 2010.
[4] J. Haunschild, J. Geilker, I.E. Reis, S. Rein, Detecting efficiency-limiting defects in Czochralski-grown silicon wafers in solar cell production using photoluminescence imaging, Physica Status Solidi RRL 5 (2011) 199.
[5] W. McMillan, T.,Trupke, J.W. Weber, In-line monitoring of electrical wafer quality using photoluminescence imaging, in: Proceedings of the 25th EU-PVSEC, Valencia, Spain, 2010.
[6] B. True, A. Stavrides, I. Latchford, Image processing techniques for correlation of photoluminescence images of as-cut wafers with final cell IV parameters, in: Proceedings of the 26th EU-PVSEC, Hamburg, Germany, 2011.
[7] H. Nagel, Luminescence Imaging—a key metrology for crystalline silicon PV, in: Proceedings of the 20th Workshop on Crystalline Silicon Solar Cells and Modules, Breckenridge, CO, USA, 2010.
[8] B. Birkmann, A. Hüsler, A. Seidl, K. Ramspeck et al., Analysis of multicrystalline wafers originating from corner and edge bricks and forecast of cell properties, in: Proceeding of the 26th EU-PVSEC, Hamburg, Germany, 2011.
[9] R. Bakowskie, R. Lantzsch, T. Kaden, K. G. Eller et al., Comparison of recombination active defects in multicrystalline Silicon by Means of photoluminescence imaging and reverse biased electroluminescence, in: Proceedings of the 26th EU-PVSEC, Hamburg, 2012.
[10] M. Demant, J. Greulich, M. Glatthaar, J. Haunschild et al., Modelling of physically relevant features in photoluminescence images, in: Proceedings of the 2nd SiliconPV—International Conference on Silicon Photovoltaics, Leuven, Belgium, 2012.
[11] B. Thaidigsmann, F. Clement, A. Wolf, E. Lohmüller et al., HIP-MWT: a simplified structure for metal wrap through solar cells with passivated rear surface, in: Proceedings of the 1st SiliconPV—International Conference on Silicon Photovoltaics, Freiburg, Germany, 2011.